The structural characterization of Co-Cu(100) superlattices by X-ray absorption spectroscopy

1994 J. Phys.: Condens. Matter 6 4981

(http://iopscience.iop.org/0953-8984/6/27/007)

J. Phys.: Condens. Matter 6 (1994) 4981–4990. Printed in the UK

The structural characterization of Co–Cu(100) superlattices by x-ray absorption spectroscopy

R Castañer†, C Prieto†, A de Andrés†, J L Martínez†, J L Martínez-Albertos‡, C Ocal‡ and R Miranda‡

† Instituto de Ciencia de Materiales de Madrid, Consejo Superior de Investigaciones Científicas, Facultad de Ciencias (C-IV), Universidad Autónoma de Madrid, E-28049 Madrid, Spain

Departamento de Física de la Materia Condensada (C-III), Universidad Autónoma de Madrid, E-28049 Madrid, Spain

Received 26 November 1993, in final form 19 March 1994

Abstract. Extended x-ray absorption fine structure has been used to determine a crystallographic distortion in the Co layers in Co–Cu single-crystal superlattices grown on Cu(100). The FCC structure of the superlattice imposed by the Cu substrate is distorted along the growing direction for the Co layers, which are compressed perpendicularly to the interfaces. They adopt the in-plane lattice constant of the Cu substrate, keeping constant the atomic volume of Co (11.30 $Å^3$/atom), close to the value for HCP-Co.

1. Introduction

The study of metallic multilayers has received increased attention in the last few years because of the wide range of physical phenomena observed in these systems. The presence of a new periodicity in artificially layered materials leads to interesting magnetic, transport and mechanical properties [1]. Nowadays, active areas of research in metallic multilayers include mirrors for soft x-rays and neutrons, giant magnetoresistence [2] and magneto-optical recording materials [3]. In particular, true superlattices (crystalline films) of magnetic–non-magnetic metals are useful systems to study in detail magnetic coupling effects and magnetotransport properties since one can correlate microstructure and magnetic properties in these well defined, model systems [4].

Unfortunately, in many cases, the understanding of the physical properties of superlattices is limited by the lack of detailed structural characterization of the samples. Diffraction techniques have been extensively used for this purpose. Thus, x-ray diffraction provides quantitative characterization of the atomic structure and disorder in metallic superlattices [5, 6], while neutron diffraction adds microscopic information on the magnetic structure of the samples [7]. In addition to diffraction experiments, structural information can also be gained by means of x-ray absorption spectroscopy (XAS). This technique is an element-specific probe of the local environment of the absorbing atom. By tuning the incoming x-ray energy, one obtains the fine structure at and above the absorption edge of the selected atom. The structural information contained in this spectrum is as follows: (i) the pre-edge structure is related to the site symmetry and valence state; (ii) the x-ray absorption near-edge structure (XANES) region contains stereochemical information (e.g. bond angles) and (iii) the extended x-ray absorption fine structure (EXAFS) gives accurate atomic distances

0953-8984/94/274981+10$19.50

and coordination numbers [8] from the absorber to its neighbours. The advantage of this technique with respect to x-ray diffraction is that, while diffraction yields information on the average structure of the two components modulated by the superlattice periodicity, EXAFS enables us to select one of them, eliminating the long-range periodicities.

In order to obtain independent information from the Co or from the Cu layers in these samples, the anomalous effect of x-ray diffraction together with a proper modelling could be performed as in [6]. Nevertheless, this kind of data has not been reported, to our knowledge, in these samples. Recently, XAS experiments [9] have been used to determine that Co layers in Co–Fe superlattices present a BCC structure for thicknesses under 20 Å. Sputtered Fe–Cu multilayers have been studied by EXAFS and it was concluded [10] that the crystalline structure of Fe layers changes, with decreasing thickness, from distorted BCC to FCC, while Cu layers always present the FCC structure. Surprisingly, the opposite conclusion (FCC-Fe and distorted BCC-Cu) has been reached from another EXAFS study of Fe–Cu superlattices prepared with a different buffer layer [11].

In this work we have studied, by XANES and EXAFS, the structural anisotropy of Co–Cu single-crystal superlattices grown on Cu(100). Spectra have been recorded varying the angle between the electric field of the x-ray beam and the layers in order to test the crystallographic anisotropy. Co–Cu(100) superlattices are of particular interest since they were shown to present an antiferromagnetic ordering at zero field [7], and, later, an oscillatory variation of the sign of the interlayer coupling [12] as a function of the Cu thickness and the largest value of negative magnetoresistance (120% at 4.2 K and 65% at room temperature) [13, 14].

2. Experimental details

The superlattices were grown under ultrahigh-vacuum conditions by alternate deposition of Co and Cu onto Cu(100) substrates. The Cu substrate was prepared by repeated cycles of Ar^+ sputtering at 1 keV and annealing at 1100 K, until a thermal energy He atom scattering (TEAS) specular beam was measurable. The number of deposited layers and the quality of the growth were also monitored *in situ* by He atom diffraction. Once the superlattices were grown, a Cu buffer layer (about 1000 Å thick) was deposited to prevent oxidation after exposure to air. More details of the growth have been reported previously [15]. The samples exhibited long-range crystalline order as evidenced by unpolarized neutron diffraction [7] and x-ray diffraction [16]. In the following we concentrate on data corresponding to a $(9Co–5Cu)_{103}$ sample, i.e. a superstructure formed by 103 periods of nine Co atomic layers and five Cu atomic layers.

Absorption experiments (EXAFS and XANES) were carried out on the XAS-3 beam line at the DCI storage ring of the Laboratoire pour l'Utilization du Rayonnement Electromagnetique (Orsay, France) with an electron beam energy of 1.85 GeV and an average current of 250 mA. Spectra of the Co and Cu K edges for the superlattices were collected with a fluorescence detection method and a fixed-exit double-crystal Si(311) monochromator was used. The incident beam intensity was measured by an ion chamber. The samples were placed into a vacuum chamber and their total fluorescence yield was measured by a photomultiplier tube with a plastic scintillator [17].

Fluorescence detection was preferred to electron yield in order to obtain information from the proper depth in the sample and also to perform the angular variation continuously. The sample has a Cu film, about 1000 Å thick, covering the superlattice, whose total thickness is about 2800 Å. An extrapolation of an Al overlayer behaviour [18] gives the result that, for a Cu overlayer of 2000 Å, the signal from the Co would be very difficult to detect by total electron yield.

Reference spectra of the HCP-Co (7 μm thick foil) and FCC-Cu (8 μm thick foil) were also measured (in transmission mode) for comparison and data analysis purposes. All spectra reported here were collected at room temperature. The energy resolution was estimated to be 2 eV from the 3d near-edge feature of the Cu foil. The energy was calibrated by setting the energy of the first maximum above the edge for the Cu foil at 8991 eV.

In order to test structural anisotropies, the experimental geometry was chosen such that the electric field $\boldsymbol{E}$ (parallel to the polarization vector) of the x-ray beam forms an angle α with respect to the layers of the superlattice (see the inset in figure 1). This angle can be changed from $\alpha = 0°$ (parallel to the layers) to $\alpha = 88°$ (nearly perpendicular to them). The incidence angle ϕ, formed between the incident x-ray wavevector and the normal to the surface of the sample, was taken to be 45° when $\alpha = 0°$. Our experimental geometry allows the sample to turn about a horizontal or vertical axis, but the axis must be always perpendicular to the incoming beam. The polarization of the x-ray beam produced at a storage ring is in the horizontal plane, so when the rotation of the sample is performed around the horizontal axis (parallel to the polarization vector) the incidence angle ϕ changes, but the angle α remains constant. Due to the monochromator characteristics, the best way to use the x-ray flow for a given resolution is to record the $\alpha = 0$ spectra within an incidence angle of $\phi = 45°$. The other spectra for angle $\alpha \neq 0$ have been recorded by turning the sample about the vertical axis. In order to study the anisotropic x-ray absorption effect we will always refer to the angle α. In order to remove the Bragg reflections due to the crystalline substrate and the superlattice from the EXAFS energy range, only specific incidence angles (and therefore angles α) were chosen.

3. Results

Figure 1 shows the normalized XANES spectra of Co and Cu for several samples recorded at different angles α. The spectra display the K-edge absorption as a function of the photon energy. The data have been normalized and shifted in order to be plotted in the same vertical scale for clarity of presentation. Note that the energy scale is different for Cu (above) and Co (below). The XANES spectrum of FCC Cu shows three peaks within 30 eV from the edge related to the $X_{4'}$, $X_{5'}$ and $L_{3'}$ critical points of the Cu bands at the Brillouin zone boundary. They represent maxima in the empty density of states of FCC Cu. XANES spectra 2 and 3 indicate that the Cu and Co layers in the superlattice, as expected, also adopt the FCC structure. The XANES spectrum of HCP Co shows a broadened peak and a shoulder instead of the second and third peaks of the FCC Cu spectrum. This illustrates the sensitivity of XANES to the different local geometries of the absorbing atoms in FCC or HCP structures.

The x-ray absorption data show the FCC structure of the Co layers in Co–Cu superlattices in accordance with other techniques. The same preparation of a Co layer over Cu(100) has been structurally studied by low-energy electron diffraction experiments and it has been shown that Co layers present a slightly distorted FCC structure [19]. The most direct evidence that Co layers in the superlattice have an FCC structure, as do the Cu ones, is given by figures 1 and 2. The existence of the same features in the XANES and EXAFS spectra for the Co layers and for the FCC Cu foil shows clearly which is the crystallographic structure. It must be noted that the position above the edge is not exactly the same due to the different distances to their coordination spheres.

Nevertheless, the amplitudes of the XANES oscillation of the Cu and Co spectra in the superlattice are considerably smaller than the corresponding ones in the foil. This fact means

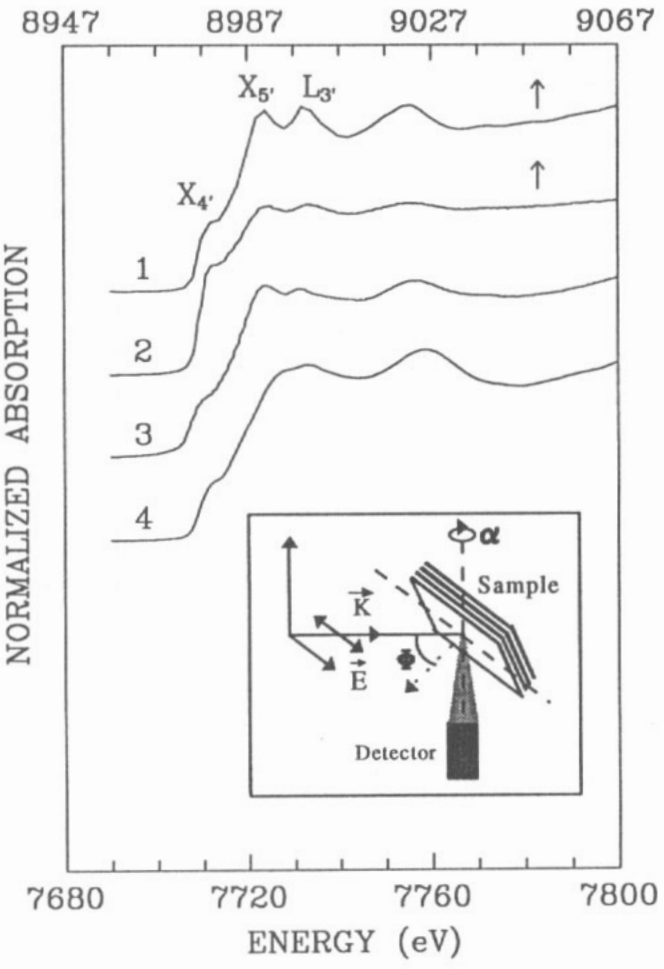

Figure 1. Normalized fluorescence XANES spectra of the Cu and Co K edges for different samples and experimental conditions. Upper scale: 1, Cu foil (transmission); 2, Cu environment in $(9Co–5Cu)_{103}$ for $\alpha = 0$. The lower energy scale refers to Co in 3, $(9Co–5Cu)_{103}$ for $\alpha = 0°$ and 4, Co foil (transmission). Upper and lower scales have been shifted for better comparison of the data. The inset shows the experimental geometry: α is the angle between the beam polarization and the layers, which is varied turning the sample about the vertical axis, and ϕ is the angle between the wave vector of the incident beam and the normal to the layers. In this figure $\alpha = 0°$ and $\phi = 45°$.

that self-absorption by the sample is observed when the fluorescence detection method is used. The sample cannot be considered as an extremely thin film or a diluted sample so the correction of the self-absorption for a concentrated sample must be applied.

A standard analysis [20] of EXAFS spectra has been carried out: the background has been removed by a cubic spline curve and the resulting data have been transformed from depending on energy to depending on wave number by $k = [2m_e/\hbar^2(E - E_0)]^{1/2}$. This yields the EXAFS interference functions $\chi_{exp}(k)$ plotted in figure 2. It can be noted that when α approaches 90° the EXAFS amplitude decreases because the self-absorption effect increases. The 'information depth' varies with the incident angle ϕ but it has been checked that the signal comes from all the layers of the superlattice. Even in the case of the Cu inside the superlattice the 'information depth' is larger than the superlattice thickness plus the 1000 Å Cu overlayer. The Cu signal reported here can be considered as that coming from a Cu(100) single crystal but obtained in the same conditions and by the same detection method as that corresponding to the Co layers. The self-absorption corrections have been

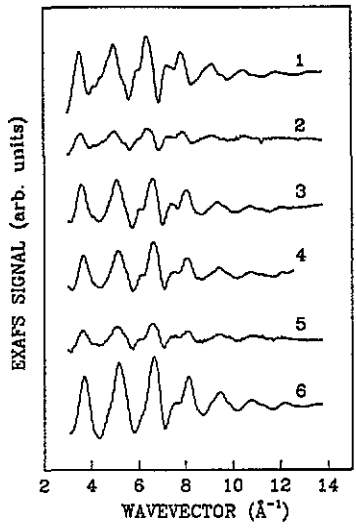

Figure 2. The $\chi(k)$ EXAFS signal extracted from fluorescence spectra, without self-absorption effect correction, of the Cu and Co K edges for different samples and experimental conditions: 1, Cu foil (transmission); 2, Cu in $(9Co–5Cu)_{103}$ ($\alpha = 0°$); 3, Co in $(9Co–5Cu)_{103}$ ($\alpha = 0°$); 4, Co in $(9Co–5Cu)_{103}$ ($\alpha = 50°$); 5, Co in $(9Co–5Cu)_{103}$ ($\alpha = 88°$); 6, Co foil (transmission).

carried out using the method described by Troger *et al* [21] in the EXAFS signal $\chi_{exp}(k)$:

$$\chi_{exp}(E) = \chi_{Co}(E)[1 - \bar{\mu}_{Co}(E)/(\mu_{tot}(E) + \bar{\mu}_{tot}(E_f)g)] = \chi_{Co}(E)[1 - S(E)] \tag{1}$$

where $\bar{\mu}_{Co}(E)$ is the absorption due to the K edge of the Co atoms, $\bar{\mu}_{tot}(E)$ is the total atomic absorption, taking into account the relative concentrations of Co and Cu in the superlattice, E is the x-ray incident energy, E_f is the fluorescence emission energy and g is the geometrical factor $g = \tan\phi$ (ϕ is the incidence angle). In a similar way, the signal from the Cu in the superlattice has been corrected, giving an EXAFS signal which is equal, within the experimental error, to that obtained from the Cu foil; this is a test that demonstrates that the correction method is correct.

The corresponding radial distribution functions (RDFs) were obtained by weighting $\chi(k)$ by the cubic wavenumber (k^3), multiplying by a Hanning window within the interval from 3.0 to 13.5 Å^{-1} and Fourier transforming. The magnitudes of the Fourier transforms of some spectra are shown in figure 3. Four well defined first coordination spheres of Co and Cu atoms in the superlattice can clearly be observed. This indicates a high degree of structural perfection in both directions, parallel and perpendicular to the layers.

These filtered EXAFS oscillations have been fitted to the well known expression [8]

$$\chi(k) = \sum_j (3N_j \cos^2\theta_j / kR_j^2) \exp(-2k^2\sigma_j^2) \exp(-\Gamma_j R_j/k) f_j(k) \sin[2kR_j + \phi_j(k)]. \tag{2}$$

(2) describes the EXAFS oscillations for a Gaussian distribution of N_j atoms at mean distances R_j around the absorbing atom considering single scattering and the plane-wave approximation. N_j is the average coordination number for the Gaussian distribution of distances centred at the value R_j, σ_j is the Debye–Waller factor, and $\phi_j(k) = 2\delta(k) + \gamma_j(k)$ is the phase shift, $\delta(k)$ and $\gamma_j(k)$ being the central and backscattering atom phase shifts,

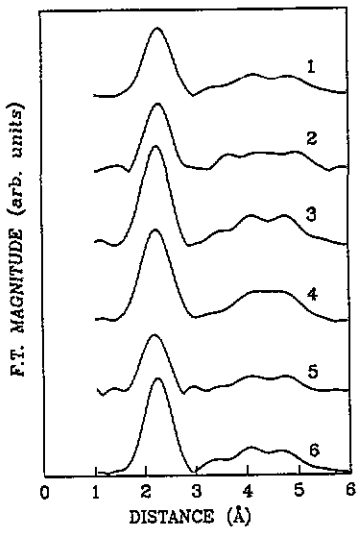

Figure 3. The magnitudes of the Fourier transforms of the $k^3\chi(k)$ weighted self-absorption effect corrected EXAFS signals. The numbers refer to the same cases as in figure 2.

respectively. $f_j(k)$ is the magnitude of the backscattering amplitude of the jth-neighbour atom; k/Γ_j is a convolution of the mean free path of the photoelectron travelling from the absorbing atom to the backscattering atoms in the jth shell and the lifetime of the core hole. The $3N_j \cos\theta_j$ term takes into account the angle θ between the polarization of the x-ray beam and the bonding direction from the absorber to the backscatterer atoms.

Synchrotron radiation is fully linearly polarized in the plane of the machine; therefore, absorption experiments can provide information on anisotropies when single crystals are studied taking advantage of this fact. The EXAFS signal is modulated by the cosine squared term, which is mathematically equivalent to a modulation of the coordination number. For polycrystalline samples, the mean value of the cosine squared is one third, which gives $\langle 3\cos^2\theta_j \rangle = 1$. This is why, in general in these cases, the polarization factor does not appear in the EXAFS expression.

In a first step, the fits were performed considering only Co–Co pair contributions in two ways: firstly, by using experimental backscattering phase and amplitude functions (transferred from the Co foil reference) and, secondly, by using the theoretical functions reported by McKale *et al* [22]. The results of this second fit are not shown because the maximum difference between the distances in the two fittings, for a given spectrum, is 0.005 Å, which can be taken as an estimation of the experimental error. In both cases, N_j has been fixed to 12, since the structure is FCC. Table 1(a) shows the EXAFS parameters from (2) after fitting the back-Fourier filtered data by usual procedures in k and R spaces. The parameter ε, defined as $\varepsilon^2 = (1/n)\sum(\text{data}_i - \text{model}_i)^2$, gives the deviation of the calculated EXAFS signals from the experimental data.

The decrease of the Fourier transform magnitude observed for $\alpha = 88°$ is consistent with a small increase in the structural disorder (σ_i) in the growth direction. The first coordination shell is different for Co atoms at the interfaces and inside the layers. It follows that the Co–Cu first-neighbour contribution to the EXAFS signal becomes maximum for $\alpha = 90°$, giving an increase of the Debye–Waller factor. Therefore, a second kind of fit has been performed, taking into account that the Co atoms placed at the interfaces between the layers have a

Table 1. A summary of the results obtained from the fits of the EXAFS spectra using (2) with both experimental and theoretical backscattering functions. (ε is the figure of merit of the fit defined in the text). (a) Only Co–Co pair contributions have been considered. The backscattering phase and amplitude functions have been obtained from the Co foil sample. (b) The Co–Co and Co–Cu pairs are taken into account to perform the EXAFS calculations. The backscattering phase and amplitude functions have been taken as those obtained by McKale *et al* [22].

(a)							
α (°)	Pair	N[a]	d (Å)	σ^2 (Å^2)	Γ (Å^{-2})	ΔE_0 (eV)	ε
0	Co–Co	12	2.517	0.0	0.0	2.35	5.29×10^{-5}
40	Co–Co	12	2.513	0.0	0.0	2.35	1.99×10^{-5}
50	Co–Co	12	2.501	0.0	0.0	2.35	3.95×10^{-5}
70	Co–Co	12	2.504	0.0	0.0	2.35	5.25×10^{-5}
78	Co–Co	12	2.502	0.0	0.0	2.35	3.95×10^{-4}
88	Co–Co	12	2.500	0.055	0.0	2.35	5.53×10^{-4}
(b)							
α (°)	Pair	$\sum 3N_j \cos\theta_j$	d (Å)	σ^2 (Å^2)	Γ (Å^{-2})	ΔE_0 (eV)	ε
0	Co–Co	11.33	2.510	0.083	0.83	−8.32	4.05×10^{-5}
	Co–Cu	0.67	2.553	0.103			
40	Co–Co	11.05	2.503	0.084	0.83	−8.32	1.24×10^{-5}
	Co–Cu	0.95	2.553	0.103			
50	Co–Co	10.95	2.493	0.084	0.83	−8.32	2.98×10^{-5}
	Co–Cu	1.05	2.553	0.103			
70	Co–Co	10.75	2.491	0.081	0.83	−8.32	2.69×10^{-5}
	Co–Cu	1.25	2.553	0.103			
78	Co–Co	10.70	2.493	0.074	0.83	−8.32	5.68×10^{-5}
	Co–Cu	1.30	2.553	0.103			
88	Co–Co	10.67	2.490	0.103	0.83	−8.32	3.75×10^{-4}
	Co–Cu	1.33	2.553	0.103			

[a] The total number of neighbours has been fixed to 12 in the fitting.

known number of Cu neighbours, which are a fraction of their first-neighbour shell. The relative coordination number is fixed and their EXAFS contribution can be easily calculated. A new fit has been made where both Co and Cu contribute to the first peak of the Fourier transform magnitude. The results are shown in table 1(b).

Figure 4 illustrates the quality of the fits; the filtered EXAFS oscillations for $\alpha = 78°$ in both k (dots) and R spaces (dots and asterisks), together with the best fit (solid line), have been plotted. In order to observe the difference, the calculated functions for the $\alpha = 0°$ best fit (dashed line) has also been plotted. The most significant result obtained from the fits (see table 1) is the decrease of the average Co–Co first-neighbour distance against angle α, as is shown in figure 5. The same trend is obtained from fits using either experimental phase shifts, for Co–Co pairs, or theoretical phases, for Co–Co and Co–Cu pairs. Since perpendicular distances to the layers are decreasingly probed at larger α, the systematic decrease of the average distance must be attributed to the lattice parameter perpendicular to the layers, which must be shorter than the parallel one. This indicates that the Co layers in the superlattice have a tetragonally distorted FCC structure, with a lattice constant perpendicular to the layers (c) shorter than that along the plane of the layers (a). In order to determine the actual extent of the tetragonal distortion, we have to realize that the $\alpha = 0°$ spectrum has contributions from four 'in-plane' and eight 'out-of-plane' neighbours, where 'in-plane' means parallel to the layers. Then the data of figure 5 result in lattice constants $a = 3.58 \pm 0.01$ Å and $c = 3.52 \pm 0.01$ Å. These values give a volume per atom of 11.30 ± 0.05 Å^3/atom. Finally, weighting each bond by its '$\cos^2\theta_j$' factor, we obtain the

dependence of the averaged distance on angle α, considering the previously desired a and c values, plotted (solid line) in figure 5, showing an excellent agreement with the experimental variation.

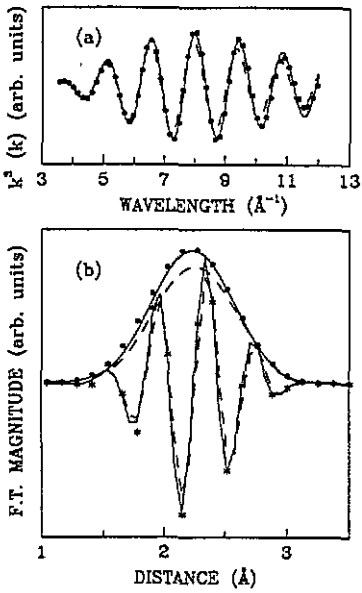

Figure 4. (*a*) A comparison of the experimental $k^3\chi(k)$ weighted EXAFS signal for the $\alpha = 78°$ spectrum (circles) and the best fit calculated by (2) assuming Co–Co and Co–Cu pairs (continuous line). The calculated EXAFS signal obtained as the best fit for the $\alpha = 0$ spectrum is also shown (dashed line). (*b*) Fourier transform modulus (circles) and imaginary part (asterisks) of the preceding signals are plotted for comparison.

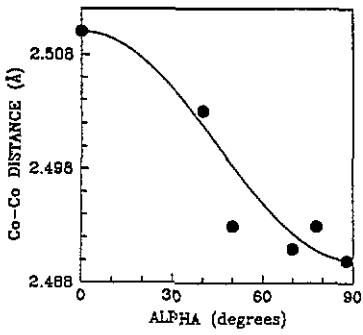

Figure 5. The first-neighbour Co–Co distance fitted with theoretical phase and amplitude backscattering functions (circles) as a function of the angle α. The continuous line is the $3\sum N_j \cos^2\theta_j$ weighted average distance for an FCT lattice with $a = 3.580$ Å and $c = 2.520$ Å.

4. Discussion

In summary, we have obtained that Co layers in the Co–Cu superlattices grown on Cu(100) substrates adopt a tetragonally distorted FCC structure, which can be termed as face centred tetragonal (FCT). The lattice parameter of the basal plane is imposed by the Cu substrate. The c parameter is reduced by an amount ($\sim$ 1.7%) consistent with the known elastic properties of Co and enough to keep an atomic volume close to that of the stable HCP phase of Co (11.10 Å^3/atom). The superlattices are coherently strained with very good in-plane lattice parameter matching, and the distortion in perpendicular distances is limited only to the Co layers.

These findings can be rationalized as follows: the lattice parameters of Cu and FCC-Co differ by 2%. Pseudomorphic growth of Co on Cu with a 2% expansion of the Co lattice in both lateral and perpendicular directions represent a large (68 meV/atom) increase in energy [23]. The tetragonal distortion of the FCC-Co layers is an attempt to minimize the energy excess that would be introduced by a uniform expansion of the lattice. By virtue of the distortion the perpendicular distances are reduced while the lateral lattice parameter of Cu is adopted by the Co layers. A recent quantitative low-energy electron diffraction (LEED) study [19] of the growth of a single film of Co on Cu(100) has shown the presence of a tetragonally distorted FCC structure with $a = 3.61 \pm 0.02$ Å and $c = 3.46 \pm 0.02$ Å up to 10 monolayers. The LEED data [19] are in excellent agreement with the lattice parameters obtained from the present EXAFS analysis. Furthermore, the dynamical LEED analysis indicates that the Co film of this thickness has not yet developed the lattice of misfit dislocations, which relax the structure of thicker films to unstrained FCC Co [24]. The existence of a tetragonal distortion has been confirmed by a recent angular-dependent SEXAFS study that reports a 2% contraction of the perpendicular spacing for Co layers 2–15 ML thick deposited on Cu(100) [25]. In that work, the reported lattice parameters ($a = 3.61 \pm 0.02$ Å and $c = 3.54 \pm 0.02$ Å, errors quoted) are also similar to ours.

An important consequence of the results shown here is that the tetragonal distortion persists for Co films covered by Cu layers and it is detectable for Co–Cu(100) superlattices. This is in contrast to other systems, such as Fe–Cu(100), where the structure of the Fe film was shown to change upon covering with Cu [26]. The implication of these subtle changes in the structure with respect to the magnetic properties is a point of much interest for future research.

Our results also seem to differ from the case of Co–Cu(111) textured multilayers where EXAFS measurements have been interpreted [27] as indicating that Co and Cu lattices are expanded and contracted, respectively, in the plane of the layers, while the lattice strain is negligible in the perpendicular direction.

5. Conclusions

We have reported EXAFS data that indicate that Co layers in $(9\text{Co}–5\text{Cu})_{103}$ single-crystal superlattices, grown on Cu(100), present a distorted FCC structure. The distortion is caused by a compression of the lattice constant along the direction perpendicular to the layers; the 'in-plane' lattice parameter remains very similar to that of the FCC Cu substrate. The atomic volume of this tetragonally distorted FCC structure is very close to that of bulk HCP-Co, which provides the explanation of the similar magnetic moment observed for the two phases in earlier measurements [7].

Acknowledgments

This work was partially supported by the CICyT under contract No MAT91-1185-E and MAT91-0588. We acknowledge the staff in charge of the DCI storage ring of LURE for allocation of beam time. Special thanks are given to P Lagarde for suggestions and a critical reading of the manuscript.

References

[1] Dhez P and Weisbuch C (ed) 1988 *Physics, Fabrication and Applications of Multilayered Structures* (New York: Plenum)
[2] Baibich M N, Broto J M, Fert A, Nguyen Van Dan F, Petroff F, Eminent P, Croquet G, Friederich A and Chazelas J 1988 *Phys. Rev. Lett.* **61** 2472
[3] Zeper W B, Greidanus F J A M, Carcia P F and Fincher C R 1989 *J. Appl. Phys.* 65 4971
[4] Falicov L M 1992 *Phys. Today* October p 46
[5] Fullerton E E, Schuller I K, Vanderstraten H and Bruynseraede Y 1992 *Phys. Rev.* B 45 9292
[6] de Santis M, de Andrés A, Raoux D, Maurer M, Ravet M F and Piecuch M 1992 *Phys. Rev.* B **46** 15 465
[7] Cebollada A, Martínez J L, Gallego J M, de Miguel J J, Miranda R, Batallán S F, Fillion G and Rebouillat J P 1989 *Phys. Rev.* B **38** 9726
[8] Teo B K 1986 *EXAFS. Basic Principles and Data Analysis* (Berlin: Springer)
Koningsberger D C and Prins R 1988 *X-ray Absorption Principles, Applications, Techniques of EXAFS, SEXAFS and XANES* (New York: Wiley)
[9] Boher P, Giron F, Houdy Ph, Baudelet F, Fontaine A, Ladouceur J M, Dartyge E, Beauvilloin P, Chappert C, Veillet P and Le Dang K 1992 *J. Appl. Phys.* 71 1798
[10] Cheng S F, Mansour A N, Teter J P, Hathaway K B and Kabacoff L T 1993 *Phys. Rev.* B 47 206
[11] Pizzini S, Baudelet F, Chanderis D, Fontaine A, Magnan H, George J M, Petroff F, Barthelemy A, Fert A, Loloee K and Schroeder P A 1992 *Phys. Rev.* B **46** 1253
[12] Cebollada A, Miranda R, Schneider C M, Schuster P and Kirschner J 1991 *J. Magn. Magn. Mater.* **102** 25
[13] Mosca D H, Petroff F, Fert A, Schroeder P A, Pratt W P and Loloee R 1991 *J. Magn. Magn. Mater.* **94** 1
[14] Parkin S S P, Li Z G and Smith D J 1991 *Appl. Phys. Lett.* **58** 2710
[15] de Miguel J J, Cebollada A, Gallego J M, Ferron J and Ferrer S 1988 *J. Cryst. Growth* **88** 442
Cebollada A, Gallego J M, de Miguel J J, Miranda R, Martínez J L, Ferrer S, Fillion G and Rebouillat J P 1990 *Vacuum* **41** 482
[16] Cebollada A 1992 *PhD Thesis* Universidad Autónoma de Madrid
[17] Tourillon G, Guay D, Lemonnier M, Bortol F and Badeyan M *Nucl. Instrum. Methods* A **294** 382
[18] Elam W T, Kirkland J P, Neiser R A and Wolf P D 1988 *Phys. Rev.* B **38** 26
[19] Navas E, Schuster P, Schneider C M, Kirschner J, Cebollada A, Ocal C, Miranda R, Cerdá J and de Andrés P 1993 *J. Magn. Magn. Mater.* **121** 65
[20] Bonin D, Kaiser P and Desbarres *'EXAFS PC-software', 8th Europhysics School Chem. Phys. (La Rabida, 1992)*
[21] Troger L, Arvanitis D, Baberschke K, Michallis H, Grimm U and Zschech E 1992 *Phys. Rev.* B **46** 3283
[22] McKale A G, Veal B W, Paulikas A P, Chan S K and Knapp G S 1988 *J. Am. Chem. Soc.* **110** 3763
[23] Marcus P M and Moruzzi V L 1988 *J. Appl. Phys.* **63** 4045
[24] Schneider C M, de Miguel J J, Bressler P, Schuster P, Miranda R and Kirschner J 1990 *J. Electron. Spectrosc. Relat. Phenom.* **51** 263
[25] Heckmann O, Magnan H, Lefevre P and Chandesris D *Surf. Sci.* submitted
[26] Magnan H, Chandesris D, Villette B, Heckmann O and Lecante J 1991 *Phys. Rev. Lett.* **67** 859
[27] Pizzini S, Baudelet F, Fontaine A, Galtier M, Renard D and Marliere C 1993 *Phys. Rev.* B **47** 8754